МІНЕРАЛОГІЧНИЙ ЖУРНАЛ
MINERALOGICAL JOURNAL
(UKRAINE)

https://doi.org/10.15407/mineraljournal.45.03.051
UDC 550.4 (477); 555.24

G.V. Artemenko, DrSc (Geology), Prof., Head of Department
E-mail: regulgeo@gmail.com; https://orcid.org/0000-0002-4528-6853
L.V. Shumlyanskyy, DrSc (Geology), Associate Professor
E-mail: lshumlyanskyy@yahoo.com; https://orcid.org/0000-0002-6775-4419
L.S. Dovbysh, Graduate Student
E-mail: dovbysh__ls@ukr.net; https://orcid.org/0000-0003-4529-448X
M.P. Semenenko Institute of Geochemistry, Mineralogy and Ore Formation of the NAS of Ukraine
34, Acad. Palladin Ave., Kyiv, Ukraine, 03142

THE AGE OF ZIRCON FROM METASEDIMENTARY ROCKS OF THE TERNUVATE STRATA (WEST AZOV BLOCK OF THE UKRAINIAN SHIELD)

In the West Azov the Ternuvate strata comprises metamorphic rocks that builds up the Haichur arcuate structure, which is about 72 km long. Its western part lies within the Andriivka fault zone, which separates the Vovcha and Huliaipole blocks, while the eastern part is located within the Ternuvate fault zone, which is traced on the Remivka block. The rocks composing the Haichur structure have irregular and laterally variable composition and changeable thickness, and show dynamometamorphic structures of boudinage and schistosity. The upper part of the Ternuvate strata is composed mainly of metasedimentary rocks — gneisses and biotite schists, garnet-biotite, magnetite-amphibole and feldspar quartzites. The lower part comprises volcanogenic rocks — amphibolites, metaultrabasites and biotite-amphibole gneisses. Using the LA-ICP-MS method, 38 zircon crystals from muscovite-biotite gneisses of the upper part of the Ternuvate strata were analyzed. According to geochemical data, they are metamorphosed greywacke. Zircon belongs to several age populations (3.65-3.45 and 3.3-2.95 Ga), corresponding to the major stages of the formation of the Archean crust in the West Azov domain, i.e., formation of the oldest basement and granite-greenstone complexes of the Paleoarchean and Mesoarchean ages. Identical populations of the detrital zircon were established in the early Precambrian metaterrigenous rocks of the Krutobalka Formation of the Sorokyne greenstone structure. The similarity of the Paleoarchean crust (3.45-3.65 Ga) of the West Azov block (Ukrainian Shield) and the Kursk-Besedine granulite-gneiss area of the Kursk Magnetic Anomaly (KMA) block is obvious, whereas the Paleoarchean and Mesoarchean complexes (3.3-2.95 Ga) correspond to the rocks of Mykhailiv and Orel-Tim granite-greenstone area of the KMA block. The Archean complexes of the Sarmatia are of the same age as similar formations of the Kaapvaal craton in South Africa, Bastar craton in India, North China Craton, Slave craton in Canada and others, which were formed since the Eoarchaean.

Keywords**:** *Haichur structure, Ternuvate sequence, muscovite-biotite gneiss, Huliaipole block, Vovcha block, Remivka block, zircon, U-Pb age, metasedimentary rocks.*

C i t e: Artemenko, G.V., Shumlyanskyy, L.V. and Dovbysh, L.S. (2023). The age of zircon from metasedimentary rocks of the Ternuvate strata (West Azov block of the Ukrainian Shield). *Mineral. Journ. (Ukraine)*, Vol. 45, No. 3, pp. 51-59. https://doi.org/10.15407/mineraljournal.45.03.051

Introduction. The Haichur arcuate structure of West Azov is a complex trough-shaped and, in its southern part, monoclinal structure extended for about 72 km [15] (Fig. 1). Its western part is located within the Andriivka fault zone, which separates the Vovcha and Huliaipole blocks, while the eastern part occurs in the Ternuvate fault zone, which is traced on the Remivka block.

The metamorphic rocks composing the Haichur structure have irregular and laterally variable composition and changeable thickness. They reveal metamorphic structures such as boudinage and schistosity. The rocks of the Haichur structure include metavolcanogenic and metasedimentary rocks, as well as granitoids strongly affected by shear-related metamorphism, and rocks of the old basement, which were displaced due to the tectonic processes. The metamorphosed volcanogenic and sedimentary rocks of the Haichur structure, which belong to the Ternuvate strata, are subdivided into two formations [9]. The upper formation (up to 800 m thick) is composed of biotite, muscovite-biotite, garnet-biotite, sillimanite-garnet, locally with cordierite, graphite, biotite-garnet, magnetite-tremolite-garnet gneisses and schists, magnetite-amphibole, feldspar, and amphibole-magnetite quartzites, amphibolites and metaultrabasites. In the eastern part of the structure, layers of amphibole-magnetite quartzites extend for 0.5-1.0 km [15].

The lower formation (up to 350 m thick) is composed of amphibolites, metaultrabasites and amphibole-biotite gneiss. The Ternuvate strata reaches its maximum thickness of 1.0 km on the eastern flankof the Haichur structure, while the

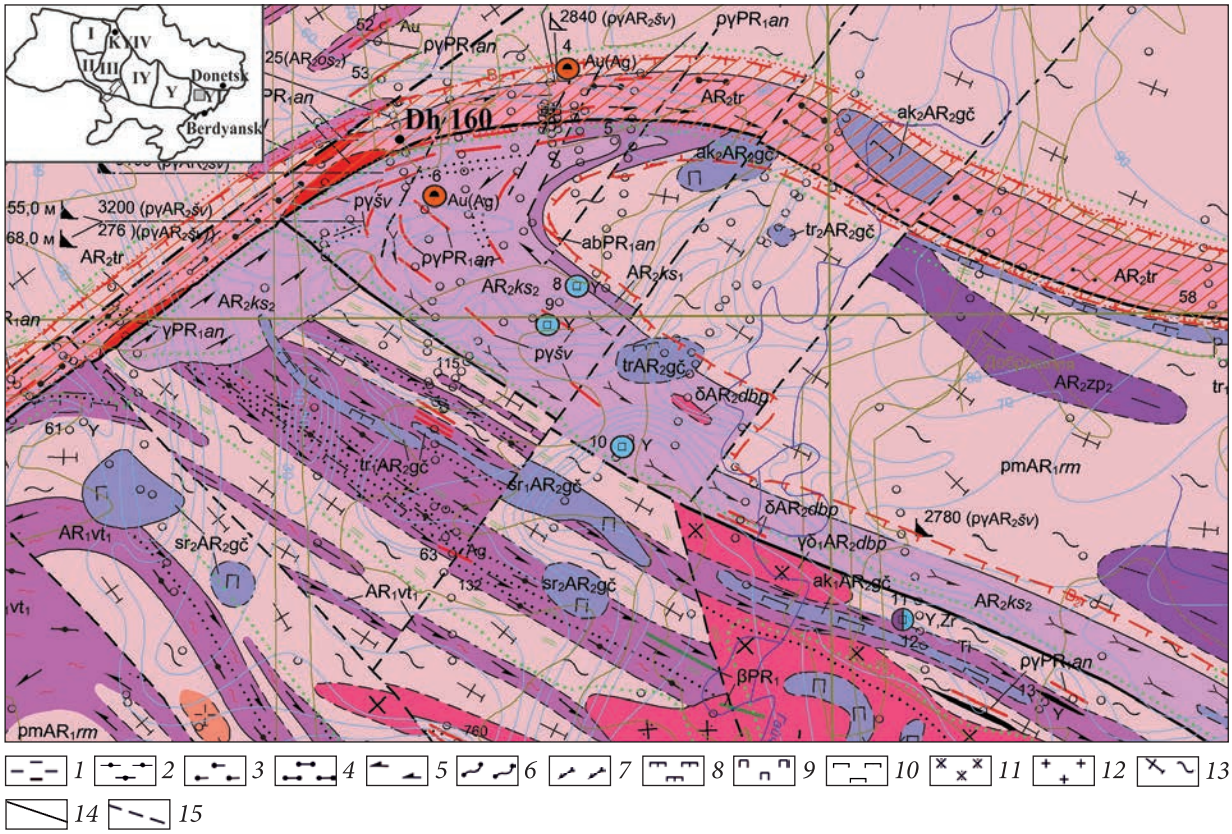

1 2 3 4 5 6 7 8 9 10 11 12 13 14 15

Fig. 1. A schematic geological map of the junction zone of the Huliaipole, Vovcha and Remivka blocks [15], with changes and additions. Plagiogneisses: *1* — biotite, *2* — amphibole-biotite, *3* — garnet-bearing biotite, *4* — garnet-biotite; *5* — amphibolites; *6* — garnet-biotite crystalline schists; *7* — amphibolites with pyroxene; *8* — tremolitites; *9* — serpentinites; *10* — actinolitites; *11* — quartz diorites; *12* — pegmatoid granites; *13* — biotite plagiomigmatites. Faults: *14* — established by direct geological observations and traced by geophysical data; *15* — established by geophysical destablished by geophysical data. Schematic map of the Ukrainian Shield. Megablocks: I — Volynian, II — Dniester-Buh, III — Ros-Tikych, IV — Ingul, V — Middle Dnieper, VI — Azov. The area of work is shown as a filled square

minimum thickness of about 100 m is observed on its western flank. Metamorphic rocks of the Ternuvate strata are cut through by Paleoproterozoic granites dated at 2.2 Ga [1]. The authors [9, 15] consider the Haichur structure as a greenstone structure similar to the Kosyvtseve greenstone belt, in which the upper terrigenous part of the section has escaped the denudation. Other authors [19] suggested that the lower part of the Ternuvate strata is composed of rocks of the West Azov Group, while the upper part belongs to the Central Azov Group.

Research objectives. We aimed at the reconstruction of the genesis and determination of the age of formation of the volcanogenic sedimentary rocks of the Ternuvate strata. Due to the strong tectonic overprint, the genesis of gneisses and schists of the Ternuvate strata is hard to establish. To determine their initial nature, the diagrams of A.A. Predovskyi (FAK) [20] and (Al_2O_3 — (K_2O + Na_2O) [21] were used. Zircon from biotite gneisses of the Ternuvate strata was dated by the LA-ICP-MS method (sample 89-227, drilhole 160, depth 149.8—154.5 m) (Fig. 2).

Research methods. Zircon has been extracted from the rock using a shaking table, heavy liquids, and a magnetic separator to produce a heavy non-magnetic fraction. Zircons were hand-picked under a binocular microscope. Zircon morphology has been studied under an optical microscope, whereas the internal structure was documented using cathodoluminescence. U-Pb isotopic data were collected using laser ablation inductively coupled plasma mass spectrometry (LA-ICP-MS) in the GeoHistory Facility, John de Laeter Centre, Curtin University. Zircon was ablated using a Resonetics RESOlution M-50A-LR system, incorporating a COMPex 102-193 nm excimer UV laser that was coupled to an Agilent 8900 QQQ mass spectrometer. Zircon standard OG1 (3465 ± 0.6 Ma [28]; all uncertainties at 2σ) was utilized as the primary reference material and analyzed in blocks with secondary standards GJ-1 (601.2 ± 0.4 Ma [13], and *Plešovice* (337.13 ± 0.37 Ma; [27]. The secondary standards yielded weighted mean $^{207}Pb/^{206}Pb$ ages and $^{238}U/^{206}Pb$ ages within an uncertainty of the recommended values. The time-resolved mass spectra were reduced using Iolite 3.7™ [18] and references therein) with final ages

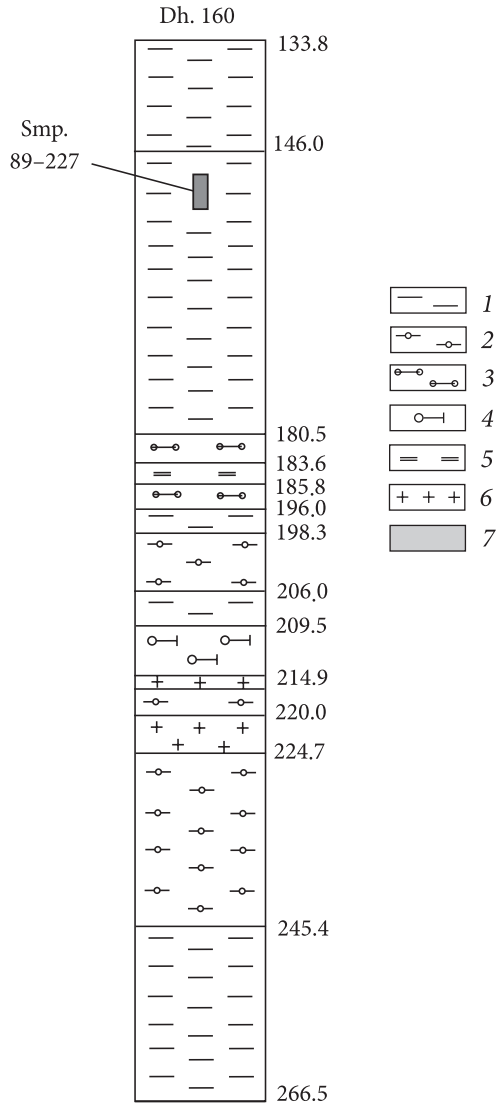

Fig. 2. Schematic log of the drilhole No. 160 after [14]: *1* — biotite and two-mica plagioclase gneiss; *2* — two-mica gneiss; *3* — two-mica sillimanite-bearing gneiss; *4* — sillimanite-garnet-biotite plagioclase gneiss; *5* — quartzite; *6* — biotite granite; *7* — sampling interval

calculated using Isoplot (Ludwig, v.4.15). Silicate rock analyses were carried out at the M.P. Semenenko Institute of Geochemistry, Mineralogy and Ore Formation (IGMOF) of the NAS of Ukraine, Kyiv.

Characteristics of the studied muscovite-biotite gneiss of the Ternuvate strata. Drilhole 160 was drilled in the northernmost part of the Haichur arcuate structure (Figs 1, 2). Beneath the weathering crust, in the depth interval of 133.8-180.5 m, muscovite-bearing biotite gneiss was recovered. It has indistinct banding, caused by the alternation of biotite-rich gneiss with

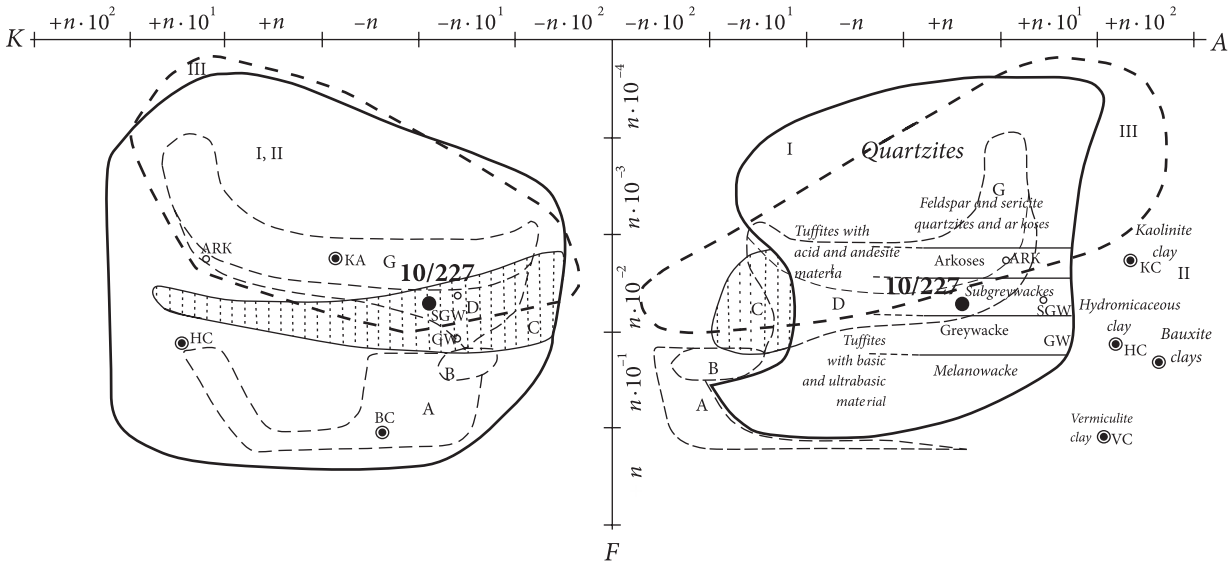

Fig. 3. The FAK diagram [20] is used for the reconstruction of the primary composition of metamorphosed aluminosilicate igneous and sedimentary rocks. Fields of sedimentary, volcanogenic-sedimentary and mixed rocks: I — sedimentary and mixed rocks; II — pelites; III — chemogenic silicites. A — ultrabasites; B — basites; C — syenites, alkaline syenites and their effusive analogues; D — diorites, plagioclase granites and their effusive analogues; G — granites and their effusive analogues. F = (FeO + MgO + Fe_2O_3) / SiO_2; A = Al_2O_3 — (CaO* + K_2O + Na_2O), where CaO* = CaO + CO_2; K = K_2O – Na_2O (in molecular units) [20]

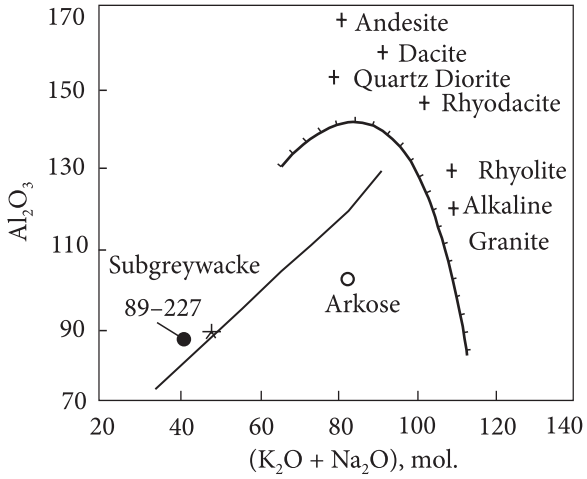

Fig. 4. Diagram Al_2O_3 – (K_2O + Na_2O) (molar amounts) for discrimination of subgreywacke from intermediate and felsic igneous rocks [21]. The trend in the diagram indicates the change of the composition of ordinary subgreywackes and arkoses with a decreasing amount of quartz

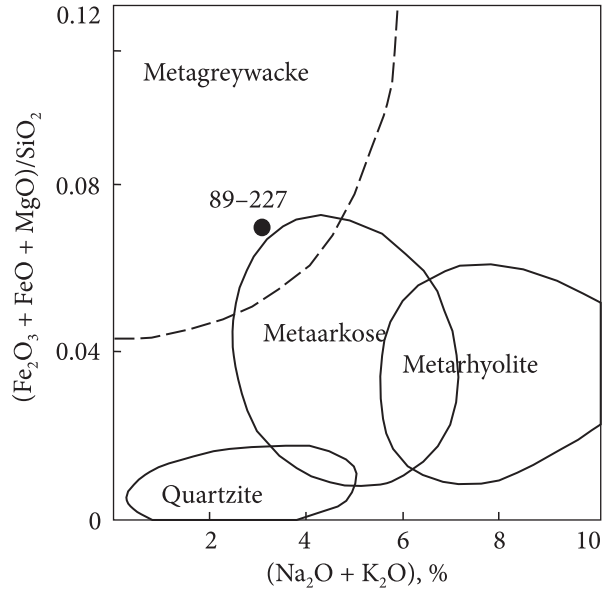

Fig. 5. Diagram (Fe_2O_3 + FeO + MgO) / SiO_2 — (Na_2O + + K_2O) for discrimination of metaarkose and metarhyolite [21]

relatively leucocratic (biotite below 10%) gneiss variety. Feldspar is rarely observed as porphyroblasts having up to 5 mm in size, or lenses up to 5×6 mm. Biotite flakes range in size from 0.5×1.0 mm to 3×5 mm. At various intervals, biotite forms clusters and the rocks attains spotted structure. The gneisses are cut by veins of aplite granite, up to 2 cm thick.

A sample 89-227 (drilhole 160, depth 149.8-154.5 m) that represent muscovite-biotite gneiss was selected for the geochronological studies. It is a light gray, fine-grained, light banded rock.

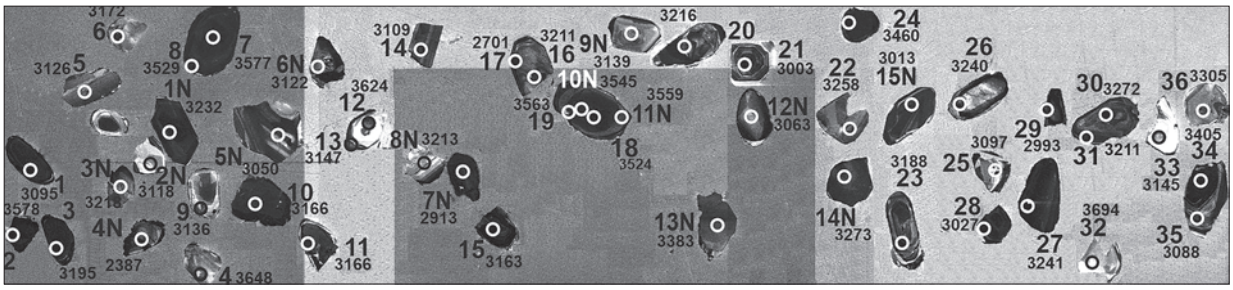

Fig. 6. FCL-images of the studied zircon crystals from muscovite-biotite gneiss of the Ternuvate strata (sample 89-227, drilhole 160, depth 149.8-154.5 m), with indicated U-Pb analysis numbers (see Table) and $^{207}Pb/^{206}Pb$ isotope age, Ma

Mineral composition (%): plagioclase — 45-60; quartz — 30-35; biotite — 10-12; muscovite — 7; opaque minerals, zircon and apatite occur in accessory amount.

This rock has high silica and a low alumina content (SiO_2 — 78.62%; TiO_2 — 0.38%; Al_2O_3 — 8.84%; Fe_2O_3 — 0.71%; FeO — 2.88%; MnO — 0.09%; MgO — 1.94%; CaO — 2.24%; Na_2O — 1.66%; K_2O — 1.40%; S_{total} — 0.10%; P_2O_5 — 0.12%; H_2O — 0.15%; LOI — 0.96%; Total — 100.09%).

In the FAK diagram [20], muscovite-biotite gneiss plot in the field of clastic aluminosilicate sedimentary rocks (subgreywackes and arkoses), which partially overlaps with the field of felsic igneous rocks of similar composition (Fig. 3). The Al_2O_3 — (K_2O + Na_2O) diagram [21] was used to distinguish subgreywacke from metamorphosed felsic and intermediate igneous rocks. In this diagram, muscovite-biotite gneiss plot in the field of subgreywackes (Fig. 4). In the diagram (Fe_2O_3 + FeO + MgO)/SiO_2 — (Na_2O + K_2O) that is used to distin-guish metaarkose and metarhyolite [21], muscovite-biotite gneiss plot in the field of metagreywacke (Fig. 5).

Zircon characterization. In the zircon fraction from muscovite-biotite gneiss (sample 89-227), several varieties of zircon were distinguished. Elongated prismatic crystals with smooth pyramids facets predominate (60%). Length of crystals along L_4 axis = 0.2-0.35 mm, elongation coefficient = 2.0-3.0. The color is pink, the luster is matte. Some grains contain dark cores. About 30% of the fraction is composed by pink zircon, more transparent, fractured, with a glassy luster and dark cores. A small amount (10%) of zircon grains are equant or elongated, length of crystals along L_4 axis = 0.15-0.35 mm, elongation coefficient = 1.0-2.5. The color of the crystals is pink, the luster is glassy, grains are transparent. The internal structure is homogeneous.

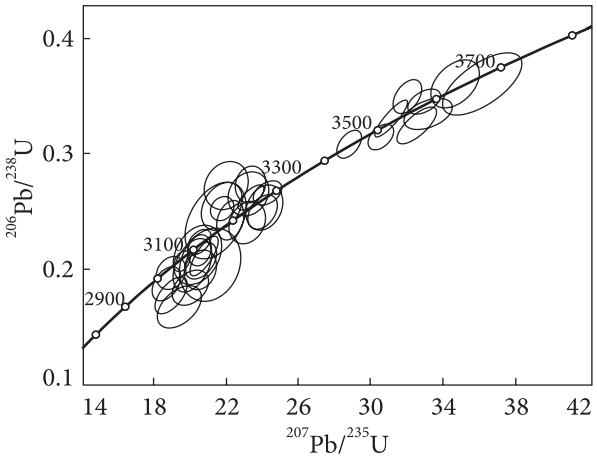

Fig. 7. U-Pb concordia diagram for zircon crystals from muscovite-biotite gneiss of the Ternuvate strata (sample 89-227). Discordant results are omitted

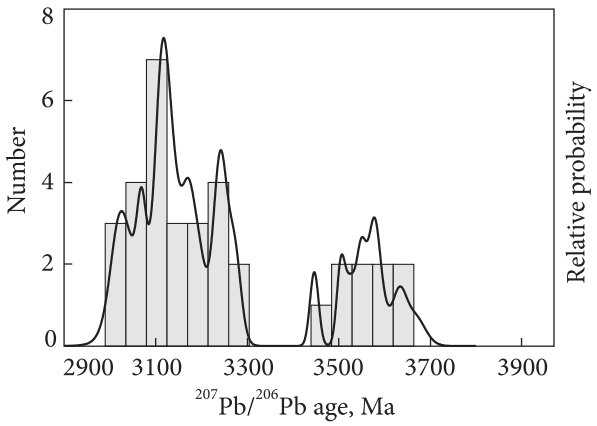

Fig. 8. The $^{207}Pb/^{206}Pb$ age distribution for detrital zircon from muscovite-biotite gneiss of the Ternuvate strata (sample 89-227). Only concordant results are plotted

Results of U-Pb dating of zircon from muscovite-biotite gneiss (sample 89-227)

# analysis	Concentration, ppm			Isotope ratio							
	U	Pb	Th	Th/U	$^{207}Pb/^{235}U$	2σ	$^{206}Pb/^{238}U$	2σ	Rho	$^{207}Pb/^{206}Pb$	2σ
1	295	205	295	2.24	19.5400	0.3700	0.6075	0.007	0.37	0.2362	0.007
2*	609	309	609	2.90	26.0000	1.2000	0.5920	0.021	0.94	0.3211	0.021
3	334	217	334	2.34	20.7700	0.6400	0.6120	0.014	0.75	0.2520	0.014
4	61	95	61	1.20	34.7000	1.1000	0.7610	0.017	0.42	0.3380	0.017
5	67	65	67	1.70	21.7500	0.9300	0.6550	0.017	0.32	0.2420	0.017
6	84	100	84	1.46	20.5800	0.7200	0.6080	0.013	0.41	0.2491	0.013
7	311	70	311	7.85	32.9800	0.7400	0.7457	0.009	0.47	0.3213	0.009
8	195	97	195	3.86	32.0500	0.6500	0.7500	0.012	0.45	0.3124	0.012
9	42	49	42	1.44	22.0000	1.0000	0.6730	0.017	0.18	0.2440	0.017
10	179	83	179	3.04	20.5100	0.5400	0.6170	0.011	0.18	0.2464	0.011
11	168	180	168	1.55	21.7700	0.5300	0.6531	0.009	0.20	0.2473	0.009
12	166	96	166	3.18	33.2000	1.1000	0.7350	0.011	0.44	0.3297	0.011
13	111	5	111	102.00	18.9400	0.7300	0.5780	0.013	0.59	0.2457	0.013
14	158	160	158	1.59	20.5100	0.5300	0.6242	0.009	0.43	0.2394	0.009
15*	386	175	386	2.82	14.7000	0.5100	0.4420	0.013	0.74	0.2478	0.013
16	102	53	102	2.97	22.2200	0.6200	0.6430	0.014	0.27	0.2522	0.014
17*	526	73	526	11.45	9.2500	0.3900	0.3760	0.015	0.89	0.1860	0.015
18	309	273	309	2.12	30.5800	0.5800	0.7150	0.009	0.45	0.3115	0.009
19	215	209	215	1.93	32.5700	0.9000	0.7250	0.013	0.73	0.3170	0.013
20	64	28	64	3.37	20.5600	0.7300	0.6000	0.014	0.20	0.2536	0.014
21*	376	164	376	2.12	11.1600	0.3100	0.3685	0.008	0.58	0.2239	0.008
22	70	92	70	1.22	23.1600	0.8300	0.6410	0.015	0.22	0.2630	0.015
23*	219	177	219	1.71	18.2700	0.4400	0.5390	0.012	0.34	0.2500	0.012
24	263	82	263	5.68	28.8200	0.5600	0.7088	0.010	0.49	0.2986	0.010
25*	192	16	192	22.30	16.6200	0.5900	0.5070	0.013	0.59	0.2393	0.013
26	81	58	81	2.82	19.4000	1.0000	0.5680	0.015	0.46	0.2550	0.015
27	265	334	265	1.35	23.3700	0.5900	0.6627	0.009	0.69	0.2579	0.009
28*	248	94	248	4.04	17.8900	0.3400	0.5813	0.007	0.05	0.2269	0.007
29*	254	62	254	5.36	8.9400	0.3500	0.2970	0.012	0.78	0.2226	0.012
30	204	333	204	1.04	24.2900	0.6500	0.6666	0.009	0.40	0.2653	0.009
31	96	196	96	0.81	23.3400	0.6900	0.6740	0.013	0.12	0.2531	0.013
32	38	25	38	3.14	36.2000	1.8000	0.7610	0.022	0.65	0.3480	0.022
33	34	18	34	3.01	20.4000	1.1000	0.6130	0.021	0.30	0.2470	0.021
34	549	460	549	2.37	31.1500	0.7400	0.7310	0.013	0.87	0.3160	0.013
35	117	85	117	2.26	18.6800	0.6500	0.5880	0.012	0.42	0.2345	0.012
36	68	105	68	1.07	24.1100	0.8400	0.6540	0.016	0.24	0.2740	0.016
1N	327	131	327	4.38	24.0162	0.6716	0.6501	0.012	0.39	0.2592	0.012
2N	49	37	49	2.10	21.1017	1.3915	0.6045	0.026	0.18	0.2503	0.026
3N*	89	79	89	1.91	19.6083	0.9806	0.5367	0.016	0.29	0.2583	0.016
4N*	543	58	543	6.27	7.5202	0.2843	0.3382	0.009	0.16	0.1560	0.009
5N	159	141	159	2.01	20.1200	0.8742	0.6040	0.019	0.42	0.2312	0.019
6N	172	141	172	2.08	20.0092	0.8234	0.5846	0.012	0.36	0.2432	0.012
7N*	113	36	113	4.96	18.8645	1.4453	0.6068	0.018	0.37	0.2200	0.018
8N*	308	115	308	2.37	14.7583	0.5440	0.4094	0.015	0.55	0.2574	0.015
9N	112	120	112	1.52	23.2307	0.9270	0.6658	0.016	0.18	0.2440	0.016
10N*	239	197	239	2.34	33.1569	1.1784	0.7386	0.015	0.35	0.3170	0.015
11N*	127	133	127	1.82	34.1972	1.2807	0.7542	0.023	0.42	0.3214	0.023
12N	50	43	50	1.79	21.4051	1.3811	0.6428	0.027	0.39	0.2371	0.027
13N*	83	139	83	1.07	25.7514	1.4202	0.6365	0.019	0.44	0.2881	0.019
14N*	84	125	84	1.21	25.5764	1.3616	0.6791	0.022	0.48	0.2667	0.022
15N	258	248	258	1.62	18.9335	0.6725	0.5974	0.012	0.21	0.2262	0.012

N o t e. Asterisk (*) indicates discordant analyses that were omitted from Fig. 7 and 8.

Isotopic age, Ma					
$^{207}Pb/^{235}U$	2σ	$^{206}Pb/^{238}U$	2σ	$^{207}Pb/^{206}Pb$	2σ
3095	27	3059	29	3068	19
3578	21	2983	87	3331	46
3195	26	3072	56	3133	31
3648	47	3643	60	3631	30
3126	70	3250	68	3160	41
3172	50	3058	50	3119	34
3577	24	3590	33	3578	22
3529	30	3609	44	3548	20
3136	77	3319	68	3178	46
3166	42	3094	44	3109	25
3166	40	3239	33	3171	24
3624	36	3553	42	3590	31
3147	47	2936	52	3030	38
3109	37	3130	36	3115	25
3163	31	2356	58	2797	34
3211	46	3196	55	3193	27
2701	36	2058	72	2382	43
3524	24	3480	34	3504	18
3563	34	3518	50	3564	29
3218	53	3026	57	3118	35
3003	37	2020	38	2533	26
3258	63	3188	60	3243	33
3188	39	2775	51	3005	23
3460	27	3452	37	3446	19
3097	49	2637	57	2906	34
3240	74	2902	64	3068	51
3231	27	3276	35	3242	24
3027	31	2953	28	2987	19
2993	38	1676	58	2331	35
3272	36	3291	33	3273	26
3211	52	3318	50	3236	29
3694	54	3639	81	3664	46
3135	89	3081	84	3123	52
3546	22	3534	49	3525	23
3088	48	2984	48	3017	34
3305	64	3245	61	3266	35
3263	27	3226	48	3232	41
3125	63	3035	102	3118	111
3075	48	2764	68	3218	72
2174	32	1876	44	2387	69
3083	43	3054	81	3050	66
3086	44	2964	51	3122	58
3005	78	3051	72	2913	113
2797	39	2207	68	3213	54
3225	39	3286	59	3139	61
3576	34	3562	55	3545	41
3605	37	3615	82	3559	56
3137	66	3207	113	3063	105
3324	58	3169	74	3383	86
3310	52	3333	83	3273	67
3037	32	3017	47	3013	46

The results of geochronological studies of zircon. The LA-ICP-MS method was applied to define the U-Pb age of zircon from muscovite-biotite gneiss of the upper formation of the Ternuvate strata. In total, 38 crystals have been dated, in which 51 age determinations have been performed (Table, Figs 6, 7, 8). Of these, 16 dates are highly discordant and omitted from farther consideration. Zircons with discordant ages have an increased content of uranium, thorium and lead. The largest number of zircon dates (24 crystals) falls within the age range of 3.3-2.95 Ga; the second most abundant population (9 crystals) is dated at the age of 3.65—3.45 Ga.

Discussion and conclusions. For the first time, a geochronological study of muscovite-biotite gneiss from the upper formation of the Ternuvate strata of the Haichur structure has been performed.

According to the chemical characteristics, this gneiss represents metamorphosed greywacke. Using the LA-ICP-MS method, 38 zircon crystals have been dated, in which 51 U-Pb age determinations have been performed. These belong to several zircon populations with the ages of 3.65-3.45, 3.3-2.95 Ga, corresponding to the major stages of the Archean crust formation in the West Azov domain, respectively to the formation of the oldest basement [2, 4, 5, 8, 17] and granite-greenstone complexes of the Paleoarchean and Mesoarchean ages [2, 26]. Similar populations of detrital zircon were established in the early Precambrian metaterrigenous rocks of the Krutobalka formation in the Soroky greenstone structure [6, 7].

Comparison of the rock associations of the Ukrainian Shield and the Kursk Magnetic Anomaly provides evidence for the similarity between the Paleoarchean crust (3.65-3.45 Ga) in the West Azov block and the Kursk-Besedine granulite-gneissic area [23, 25], whereas the Mesoarchean complexes (3.3-2.95 Ga) correspond to the rocks of Mykhailiv and Orel-Tim granite-greenstone area of the Kursk Magnetic Anomaly [3, 24].

The Archean complexes of the Sarmatia are of the same age as similar formations of the Kaapvaal craton in South Africa [16], Bastar craton in India [10, 22], North China Craton [29], Slave craton in Canada [11, 12], which have been formed since the Eoarchean.

REFERENCES

1. Artemenko, G.V., Samborska, I.A., Shvaika, I.A., Gogolev, K.I. and Dovbush, T.I. (2018), *Mineral. Journ. (Ukraine)*, Vol. 40, No. 2, Kyiv, UA, pp. 45-62 [in Russian]. https://doi.org/10.15407/mineraljournal.40.02.045
2. Artemenko, G.V. and Shumlyanskyy, L.V. (2021), *Geol. Journ*., No. 3, Kyiv, UA, pp. 35-47. https://doi.org/10.30836/igs.1025-6814.2021.3.228873
3. Artemenko, G.V., Shumlyanskyy, L.V., Bekker, A.Yu. and Hoffman, A. (2022), *Geochemistry and ore formation*, Vol. 43, Kyiv, UA, pp. 3-11 [in Ukrainian]. https://doi.org/10.15407/gof.2022.43.003
4. Artemenko, G.V., Shumlyanskyy, L.V. and Shvaika, I.A. (2014), *Geol. Journ*., No. 4 (349), Kyiv, UA, pp. 91-102 [in Russian]. https://doi.org/10.30836/igs.1025-6814.2014.4.139191
5. Artemenko, G.V., Shumlyanskyy, L.V., Wilde, S.A., Whitehouse, M.J. and Bekker, A.Yu. (2021), *Geol. Journ*., No. 1 (374), Kyiv, UA, pp. 3-16. https://doi.org/10.30836/igs.1025-6814.2021.1.216989
6. Bibikova, E.V., Claesson, S., Fedotova, A.A., Artemenko, G.V. and Ilyinsky, L. (2010), *Geochem. Int*., Vol. 48, pp. 845-861. https://doi.org/10.1134/S0016702910090016
7. Bibikova, E., Fedotova, A., Claesson, S., Anosova, M. and Shumlyanskyy, L. (2013), in: *Problems of the Origin and Evolution of the Biosphere*, Krasand publ., Moscow, pp. 147-167 [in Russian].
8. Bibikova, E.V. and Williams, I.S. (1990), *Precam. Res*., Vol. 48, Iss. 3, pp. 203-221. https://doi.org/10.1016/0301-9268(90)90009-F
9. Esypchuk, K.Yu., Bobrov, O.B., Stepanyuk, L.M., Shcherbak, M.P., Glevaskiy, E.B., Skobelev, V.M., Drannik, V.S. and Geichenko, M.V. (2004), *Correlated chronostratigraphic scheme of Early Precambrian of the Ukrainian Shield (scheme and explanatory note)*, UkrSGRI, NSC Ukraine, Kyiv, UA, 30 p. [in Ukrainian].
10. Ghosh, J.G. (2004), *J. Asian Earth Sci*., Vol. 23, Iss 3, pp. 359-364. https://doi.org/10.1016/S1367-9120(03)00136-6
11. Iizuka, T., Komiya, T., Ueno, Y., Katayama, I., Uehara, Y., Maruyama, S., Hirata, T., Johnson, S.P. and Dunkley, D.J. (2007), *Precam. Res*., Vol. 153, pp. 179-208. https://doi.org/10.1016/j.precamres.2006.11.017
12. Iizuka, T., Komiya, T., Johnson, S.P., Kon, Y., Maruyama, S. and Hirata, T. (2009), *Chem. Geol*., Vol. 259, pp. 230-239. https://doi.org/10.1016/j.chemgeo.2008.11.007
13. Jackson, S.E., Pearson, N.J., Griffin, W.L. and Belousova, E.A. (2004), *Chem. Geol*., Vol. 211, Iss. 1-2, pp. 47-69. https://doi.org/10.1016/j.chemgeo.2004.06.017
14. Kiktenko, V.F. (1982), *Deep geological mapping at a scale smaller than* 1:200 000 *within sheets* M-37-XXXI, /-37-I, VII (Western Azov region - sheets M-37-133; M-37-134-B; /- 37-1; /- 37-2; /-37-13; /- 37-14; /- 37-25-A, B; /- 37-26-A, B), Kyiv, UA [in Russian].
15. Kinshakov, V.N. (1990), *Deep geological mapping at a scale* 1 : 50 000, carried out in 1986-1990. Sheets L-37-1-B, L-37-1-G, Kyiv, UA [in Russian].
16. Kroner, A. (2007), ***D****evelopments in Precamb. Geol*., Vol. 15, pp. 465-480. https://doi.org/10.1016/S0166-2635(07)15052-0
17. Lobach-Zhuchenko, S.B., Bibikova, E.V., Balagansky, V.A., Sergeev, S.A., Artemenko, G.V., Arestova, N.A., Shcherbak, N.P. and Presnyakov, S.L. (2010), *Dokl. Earth Sci*., Vol. 433(1), pp. 873-878. https://doi.org/10.1134/S1028334X10070068
18. Paton, C., Hellstrom, J., Paul, B., Woodhead, J. and Hergt, J. (2011), *J. Anal. At. Spectrom*., Vol. 26, pp. 2508-2518. https://doi.org/10.1039/C1JA10172B
19. Pereverzev, S.I. (1989), *Geol. Journ*., No. 4, Kyiv, UA, pp. 56-64 [in Russian].
20. Predovsky, A.A. (1970), *Geochemical reconstruction of the primary composition of metamorphosed volcanogenic-sedimentary formations of the Precambrian*, Apatity, RU, 115 p. [in Russian].
21. Predovsky, A.A. (1980), *Reconstruction of the conditions of sedimentogenesis and volcanism of the Early Precambrian*, Nauka, Leningrad, RU, 152 p. [in Russian].
22. Rajesh, H.M., Mukhopadhyay, J., Beukes, N.J., Belyanini, G.A. and Armstrong, R.A. (2009), *J. Geol. Soc*., Vol. 166, pp. 193-196. https://doi.org/10.1144/0016-76492008-089
23. Savko, K.A., Samsonov, A.V., Chervyakovskaya, M.V., Korish, E.Kh., Larionov, A.N. and Bazikov, N.S. (2020), *Bull. Voronezh State Univ., Ser. Geol*., No. 3, Voronezh, RU, pp. 30-44 [in Russian]. https://doi.org/10.17308/geology.2020.3/3007
24. Savko, K.A., Samsonov, A.V., Larionov, A.N., Korish, E.Kh., Chervyakovskaya, M.V. and Bazikov, N.S. (2019), *Materials of the LI Tectonic Meeting*, Vol. 2, GEOS publ., Moscow, RU, pp. 270-273 [in Russian].
25. Savko, K.A., Samsonov, A.V., Larionov, A.N., Chervyakovskaya, M.V., Korish E.Kh., Larionova, Y.O., Bazikov, N.S. and Tsybulyaev, S.V. (2021), *Precam. Res*., Vol. 353, 106021. https://doi.org/10.1016/j.precamres.2020.106021
26. Shcherbak, N.P., Artemenko, G.V., Lesnaya, I.M. and Ponomarenko, A.N. (2005), *Geochronology of the Early Precambrian of the Ukrainian Shield*. *Archaean*, Nauk. dumka, Kyiv, UA, 242 p. [in Russian].
27. Sláma, J., Košler, J., Condon, D.J., Crowley, J.L., Gerde, A., Hanchar, J.M., Horstwood, M.S., Morris, G.A., Nasdala, L. and Norberg, N. (2008), *Chem. Geol*., Vol. 249, Iss. 1-2, pp. 1-35. https://doi.org/10.1016/j.chemgeo.2007.11.005
28. Stern, R.A., Bodorkos, S., Kamo, S.L., Hickman, A.H. and Corfu, F. (2009), *Geostand. Geoanal. Res*., Vol. 33(2), pp. 145-168. https://doi.org/10.1111/j.1751-908X.2009.00023.x

29. Wan, Y.S., Liu, D.Y., Dong, C.Y., Xie, H.Q., Kröner, A., Ma, M.Z., Liu, S.J., Xie, S.W. and Ren, P. (2015), *Precambrian Geology of China*, in Zhai, M. (ed.), Springer Geology. Springer, Berlin, Heidelberg, pp. 59-136. https://doi.org/10.1007/978-3-662-47885-1_2

Received 14.04.2023

Г.В. Артеменко, д-р геол. наук, проф., зав. відділу
E-mail: regulgeo@gmail.com; https://orcid.org/0000-0002-4528-6853
Л.В. Шумлянський, д-р геол. наук, доц., пров. наук. співроб.
E-mail: lshumlyanskyy@yahoo.com; https://orcid.org/0000-0002-6775-4419
Л.С. Довбиш, аспірант
E-mail: dovbysh__ls@ukr.net; https://orcid.org/0000-0003-4529-448X
Інститут геохімії, мінералогії та рудоутворення ім. М.П. Семененка НАН України
03142, м. Київ, Україна, просп. Акад. Палладіна, 34

ВІК ЦИРКОНУ З МЕТАОСАДОВИХ ПОРІД ТЕРНУВАТСЬКОЇ ТОВЩІ (ЗАХІДНОПРИАЗОВСЬКИЙ БЛОК УКРАЇНСЬКОГО ЩИТА)

На Західному Приазов'ї тернуватська товща метаморфічних порід складає Гайчурську структуру дугоподібної форми довжиною орієнтовно 72 км. Її західна частина знаходиться в зоні Андріївського розлому, який розділяє Вовчанський і Гуляйпільський блоки, а східна — у зоні Тернуватського розлому на Ремівському блоці. Породи, які складають Гайчурську структуру, характеризуються строкатим та мінливим за латераллю складом і змінною потужністю, у них спостерігаються динамоструктури — розлінзування та розсланцювання. Верхня світа тернуватської товщі складена переважно метаосадовими породами — гнейсами та сланцями біотитовими, гранат-біотитовими, глиноземистими, магнетит-амфіболовими і польовошпатовими кварцитами. Нижня світа представлена вулканогенними породами — амфіболітами, метаультрабазитами і гнейсами біотит-амфіболовими. Методом *LA-ICP-MS* було датовано 38 кристалів циркону з мусковіт-біотитових гнейсів верхньої світи тернуватської товщі, які за петрохімічними даними відповідають метаморфізованим граувакам. Серед них виявлено популяції циркону — 3,65—3,45 та 3,3—2,95 млрд рр., які відповідають етапам формування архейської кори Західноприазовського домена — утворенню найдавнішого фундаменту та граніт-зеленокам'яних комплексів палеоархейського і мезоархейського віку (відповідно). Аналогічні популяції детритового циркону були визначені у ранньодокембрійських породах крутобалкінської світи у Сорокинській зеленокам'яній структурі. Зіставлення породних асоціацій Українського щита і Курської магнітної аномалії (КМА) унаочнює відповідність палеоархейської кори (3,45—3,65 млрд рр.) Західноприазовського блоку і Курсько-Бесединської грануліт-гнейсової області, а палеоархей-мезоархейських комплексів (3,3—2,95 млрд рр.) — породам Михайлівської і Орловсько-Тимської структур гранітно-зеленокам'яної області КМА. Архейські комплекси Сарматського континенту є одновіковими до подібних утворень кратону Каапвааль у Південній Африці, кратону Бастар в Індії, Північно-Китайського кратону, кратону Слейв у Канаді та інших, що сформувались, починаючи з еоархею.

Ключові слова: Гайчурська структура, тернуватська товща, мусковіт-біотитовий гнейс, Гуляйпільський блок, Вовчанський блок, Ремівський блок, циркон, U-Pb вік, метаосадові породи.